Simulation of Spin-Polarized Transport in Submicrometer Device Structures

Semion Saikin[a,b,c], Min Shen[a], Ming-C. Cheng[a], Vladimir Privman[a,b]
[a]Center for Quantum Device Technology, Department of Electrical and Computer Engineering and
[b]Department of Physics, Clarkson University, Potsdam, New York, 13699-5720, USA
[c]Department of Physics, Kazan State University, Russian Federation
[c]Electronic mail: saikin@clarkson.edu

Abstract: **The Monte Carlo approach is utilized to study spin-polarized electron transport in spintronic device structures. Evolution of the electron spin polarization vector is controlled by the spin-orbit interaction. Spin polarization properties, including the spin-dephasing length and orientation of the polarization vector, are investigated, for the applied voltage from 0.05V to 0.25V, and for temperatures ranging from 77K to 300K.**

Keywords: Monte Carlo, spin relaxation, spintronics, polarization

I. INTRODUCTION

Since the pioneering proposal of the spin-FET by Datta and Das [1], many devices utilizing spin dependent phenomena in semiconductors have been investigated [2-7]. Spintronic devices hold promise of reduced power consumption, faster operation and smaller size. In comparison with conventional microelectronic devices, detailed spin-dependent transport parameters are still not well studied [8]. In order to understand the spin dependent transport, realistic models are needed. The Monte Carlo simulation approach incorporating evolution of the electron spin polarization vector [9-12] is the one of the possible tools can provide physical insight into and parameter values for spin-polarized transport in spintronic devices. It goes beyond the approximations of the drift-diffusion and hydrodynamic transport models.

Monte Carlo simulation has been used to study spin transport parameters in the asymmetric single quantum well (QW) structure shown in Figure 1. Such structures have been proposed as components of different spin-FET designs [1,6,7]. In comparison with triangular QWs [1], this device structure allows suppression of influences of the excited subbands by varying the QW width. Experimental realizations of spin-FET structures are presently in progress [13]. We hope that the model described in the present study will be useful in interpreting the experimental results.

II. MODEL OF SPIN-POLARIZED TRANSPORT

In the considered device structure, shown in Figure 1, spatial motion of electrons is simulated within the traditional Monte Carlo scheme for 2D electron transport [14], where motion in the z direction is quantized, while transport in the xy plane is assumed to be semiclassical. Electron spins are described by the spin density matrix [15],

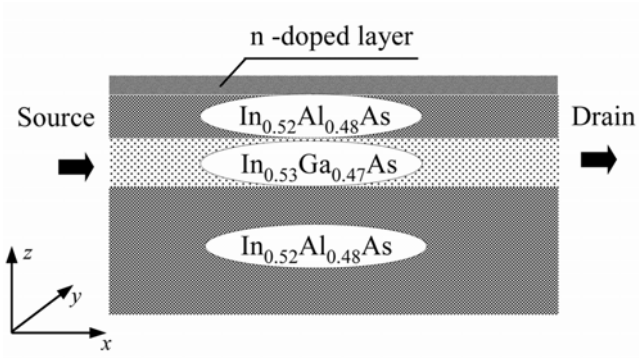

Figure 1. Device channel structure.

$$\rho = \begin{pmatrix} \rho_{\uparrow\uparrow} & \rho_{\uparrow\downarrow} \\ \rho_{\downarrow\uparrow} & \rho_{\downarrow\downarrow} \end{pmatrix}. \qquad (1)$$

The diagonal terms in (1) are the (real, nonnegative) probabilities to find an electron in spin-up and spin-down states along the z axis. The off-diagonal terms, which are complex-conjugate of each other, define the degree of quantum superposition between up and down states.

To calculate the current spin polarization at the position **r**, we average the density matrices for all the electrons located in a small volume $d^3\mathbf{r}$ near **r**, and moving with the in-plane wavenumber in the inverse-area $d^2\mathbf{k}$ near **k**. This description is possible because the spatial motion is treated as classical, with momentum $\hbar\mathbf{k}$. The averaged spin density matrix, $\langle\rho(\mathbf{r},\mathbf{k},t)\rangle$, is then an analog of a distribution function for spin-polarized electrons. It can be projected onto the Pauli matrix space using $f_\alpha = Tr(\sigma_\alpha\langle\rho\rangle)$, where σ_α is the set of the three Pauli matrices, $\alpha = x,y,z$, plus the diagonal matrix ½, which corresponds to the non-polarized state ($\alpha = n$). Similarly to the quantities defined as moments of the non-polarized electron distribution function, f_n, one can get the spin density, $n_\alpha(\mathbf{r},t)$, spin current density components, $j_\alpha(\mathbf{r},t)$, etc., as moments of the functions $f_{x,y,z}$. In this work, present only the steady state results, for the set of the zeroth-order moments

Published in Proc. Conference "IEEE-NANO 2003" (IEEE Press, Monterey, CA, 2003), Pages 91-94.

normalized by the local electron density, $S_\alpha(\mathbf{r}) = n_\alpha(\mathbf{r})/n_n(\mathbf{r})$, which yield the components of the spin polarization vector. The spin-polarization vector $\mathbf{S}(\mathbf{r})$ satisfies $|\mathbf{S}(\mathbf{r})| \le 1$. It is equal to 1 for completely spin-polarized current, and 0 for non-polarized current.

In the absence of external magnetic fields, at high temperatures, the electron spin evolution in the considered structure is controlled mainly by the spin-orbit interaction. This interaction has been traditionally described by the Dresselhaus mechanism [16]

$$H_D = \beta\left\langle k_z^2 \right\rangle (k_y\sigma_y - k_x\sigma_x), \quad (2)$$

and the Rashba mechanism [17],

$$H_R = \eta(k_y\sigma_x - k_x\sigma_y). \quad (3)$$

Each momentum scattering event changes the spin-orbit interaction and influences the subsequent electron spin evolution. The evolution of the electron spin density matrix during transport in the channel, along the classical trajectory, between the momentum-change Monte Carlo-simulation events, is described by

$$\rho(t+dt) = e^{-iH_{SO}(\mathbf{k})dt/\hbar}\rho(t)e^{iH_{SO}(\mathbf{k})dt/\hbar}, \quad (4)$$

where $H_{SO} = H_R + H_D$, and the momentum $\hbar\mathbf{k}$ is changed by the scattering events and by the electric field. Details of the model are described in [11]. The variation of a current spin polarization vector along the channel can be represented as coherent rotation and depolarization (loss of magnitude).

For the considered device structure, see Figure 1, we assume that the equilibrium two-dimensional electron density is $N_s = 0.9\cdot10^{12}$ cm^{-2}. The length of the device channel is $L_D = 0.55$ microns. The width of the QW is $w = 15$ nm, and the electric field in it, induced by the donor layer, is assumed to be constant along the channel, $\langle E_z \rangle = 240$ kV/cm. The conduction band parameters for $In_{0.53}Ga_{0.47}As$ were taken from [18]. The spin-orbit coupling constants are crucial parameters for simulation of the spin polarization. Experimentally estimated values vary widely. Here the Rashba coupling constant was estimated $\eta = 0.576\cdot10^{-9}$ eV/cm, using the expression given in [19], while the Dresselhaus constant, $\beta = 0.644\cdot10^{-22}$ eV/cm^3, was interpolated from [20, 21].

III. SIMULATION AND DISCUSION

The drain-source voltage, $V_{DS} = 0.05 - 0.25$ V, is applied along the channel. The calculated average energy profiles in the device channel for different values of V_{DS} are shown in Figure 2. Electrons injected at the left boundary are assumed thermalized, and the right boundary is completely absorbing.

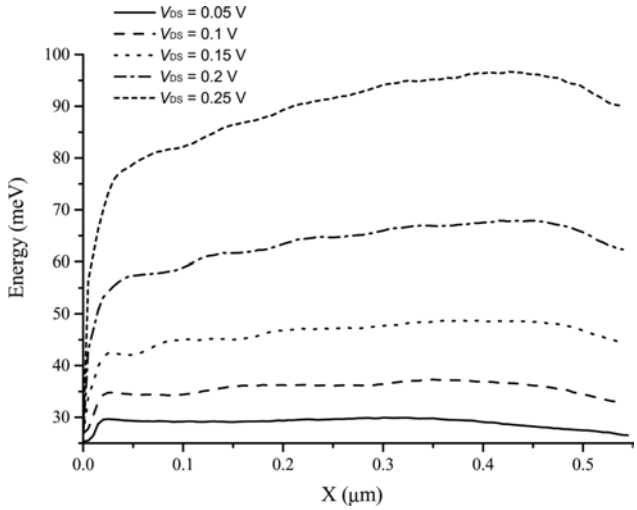

Figure 2. Energy profiles for T=300 K.

Within a small distance from the injection boundary, $l \approx 0.05$ microns, electrons strongly accelerate up to energies such that the optical phonon emission scattering mechanism becomes dominant. Transport in the rest of device is almost drift-diffusive.

The simulation program allows definition of any direction and degree of spin polarization for the injected electrons. However, in this work we consider the injected spin oriented along the channel direction [1]. Moreover, the injected current is assumed completely polarized. The current loses its polarization on the scale of characteristic spin scattering length, see Figure 3.

While the spin-FET proposed by Datta and Das [1] functions within the ballistic regime that requires $L_D << L_{SS}$, for the device-size and spin-scattering lengths, the spin-FET studied by Schliemann, Egues and Loss [6] operates in the regime of the spin scattering length varying from $L_{SS} << L_D$ to $L_{SS} >> L_D$, by tuning the spin-orbit coupling constants. The calculated spin scattering length in the considered device for temperatures $T = 77 - 300$ K is in the deep submicron length scale, as shown in Figure 3, which is consistent with the experimental results [13], where possible spin dependent effects in a micron size device disappear above $T = 190$ K. In the considered temperature diapason, the spin scattering length can be approximately described by a linear function, as shown in Figure 3.

To provide a more detailed description of the evolution of the spin depolarization, the magnitude and components of $\mathbf{S}(x)$ in the spin device channel are displayed in Figures 4(a) and 4(b), for two different choices of the coupling constants for the spin-orbit interaction. Due to specific symmetry of the spin-orbit interaction, the spin dephasing rate depends on the instantaneous orientation of polarization vector. This results in the oscillatory behavior for $|\mathbf{S}(x)|$, as seen in Figure 4.

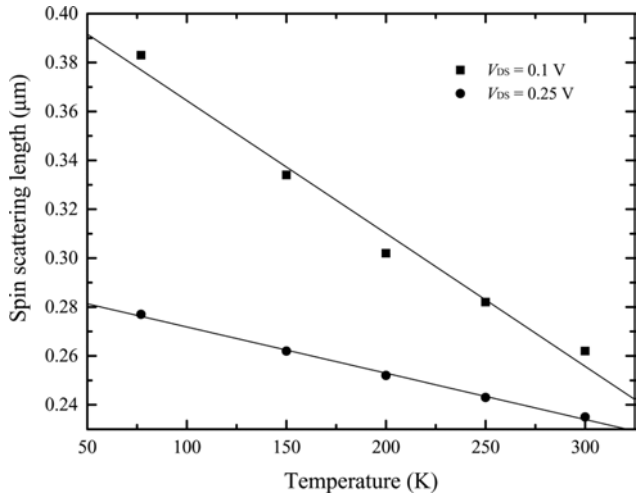

Figure 3. Spin scattering length as a function of the temperature.

In addition to the spin scattering length, one of the important characteristics of spintronic devices is the orientation of the spin-polarization vector. It controls the selective filtering of the spin-polarized current across a semiconductor/ferromagnetic interface [22]. In the ideal case, the Rashba mechanism is much stronger than the Dresselhaus mechanism, i.e., $\eta >> \beta\langle k_z^2 \rangle$, where $\langle k_z^2 \rangle$ is determined by the shape of confining potential. Consequently, the spin polarization only rotates in the *xz* plane, as displayed in Figure 4(a). When the Dresselhaus constant is increased, see Figure 4(b), the spin rotation in the *yz* plane is substantially enhanced. Two angles can be introduced to describe the spin rotation, as defined in Figure 5, where the orientation of the polarization vector at the device drain boundary is shown. While the rotation angle in the *yz* plane, θ, is relatively small at different drain-source voltages, the rotation angle in the *xz* plane, ϕ, varies up to 90° for 0.05V < V_{DS} < 0.25V.

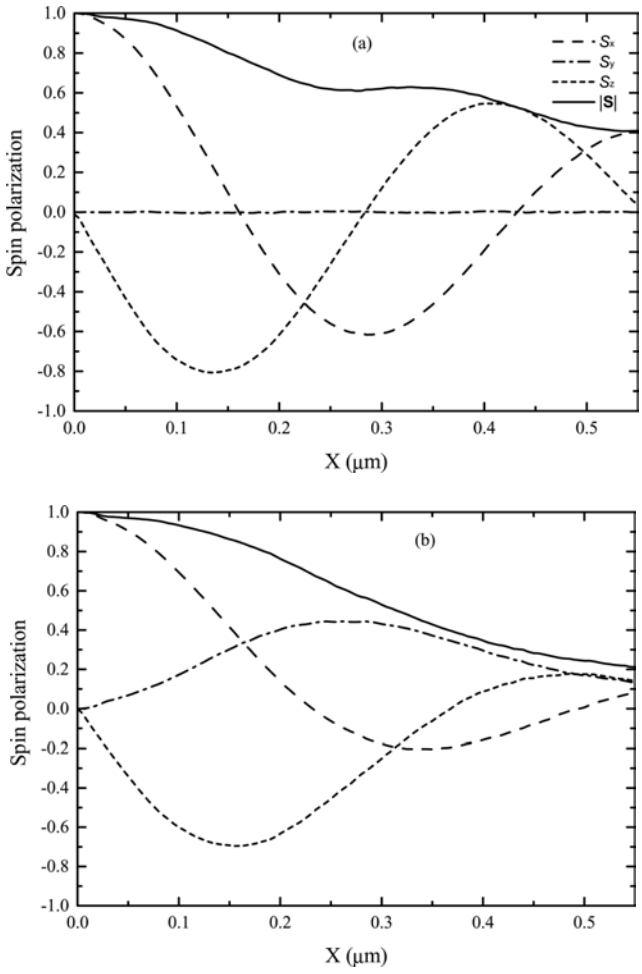

Figure 4. Evolution of the spin-polarization vector at T = 77 K, V_{DS} = 0.1 V, for two different choices of the spin-orbit coupling constants: (a) parameters from [23], (b) parameters calculated in this work.

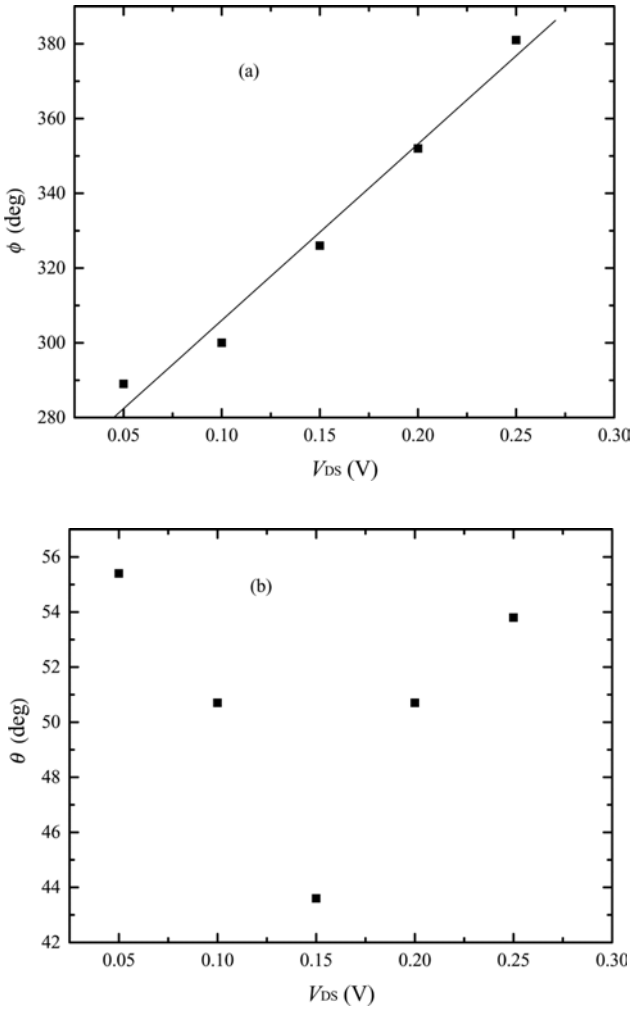

Figure 5. Orientation of the spin polarization vector at the drain boundary, at T = 77 K. The angle ϕ is measured in the *xz* plane, from the *x* axis, and θ is measured in the *yz* plane, from the *y* axis.

IV. CONCLUSIONS

We developed a new Monte Carlo approach for simulation of spin-polarized current in two-dimensional device structures. Spin-dependent parameters, including spin scattering length and orientation of the spin polarization vector, have been studied at the applied voltages from 0.05V to 0.25V and temperatures from 77K to 300K.

The calculated values of the spin scattering length range from 0.2 to 0.4 μm for different values of the temperature and drain-source voltage. We found that the spin scattering length is dependent approximately linearly on the temperature. The rotation of the polarization vector depends significantly on the applied voltage and the chosen Rashba and Dresselhaus coupling values.

REFERENCES

[1] S. Datta, B. Das, "Electronic analog of the electro-optic modulator," Appl. Phys. Lett., vol. 56, pp.665–667, 1990.

[2] M. E. Flatte, G. Vignale, "Unipolar spin diodes and transistors," Appl Phys. Lett., vol. 78, pp. 1273–1275, 2001.

[3] I. Zutic, J. Fabian, S. Das Sarma, "Proposal for a spin-polarized solar battery," Appl. Phys. Lett., vol. 79, pp. 1558–1560, 2001.

[4] T. Koga, J. Nitta, H. Takayanagi, "Spin-filter device based on the Rashba effect using a nonmagnetic resonant tunneling diode," Phys. Rev. Lett., vol. 88, art. no. 126601, 2002.

[5] X. F. Wang, P. Vasilopoulos, F. M. Peeters, "Spin-current modulation and square-wave transmission through periodically stubbed electron waveguides," Phys. Rev. B, vol. 65, art. no. 165217, 2002.

[6] J. Schliemann, J. C. Egues, D. Loss, "Nonballistic spin-field-effect transistor," Phys. Rev. Lett., vol. 90, art. no. 146801, 2003.

[7] J. C. Egues, G. Burkard, D. Loss, "Datta-Das transistor with enhanced spin control," Appl. Phys. Lett., vol. 82, pp. 2658–2660, 2003.

[8] S. A. Wolf, D. D. Awschalom, R. A. Buhrman, J. M. Daughton, S. von Molnar, M. L. Roukes, A. Y. Chtchelkanova, D. M. Treger, "Spintronics: a spin-based electronics. Vision for the future," Science, vol. 294, pp. 1488–1495, 2001.

[9] A. Bournel, V. Delmouly, P. Dollfus, G. Tremblay, P. Hesto, "Theoretical and experimental considerations on the spin field effect transistor," Physica E, vol. 12, pp 86–90, 2001.

[10] A. A. Kiselev, K. W. Kim, "Progressive suppression of spin relaxation in two-dimensional channels of finite width," Phys. Rev. B, vol. 61, art. no. 13115, 2000.

[11] S. Saikin, M. Shen, M.-C. Cheng, V. Privman, "Semiclassical Monte Carlo model for in-plane transport of spin-polarized electrons in III-V heterostructures," J. Appl. Phys., in press, 2003.

[12] S. Pramanik, S. Bandyopadhyay, M. Cahay, "Spin dephasing in quantum wires," Phys. Rev. B, in press, 2003.

[13] Y. Sato, S. Gozu, T. Kita, S. Yamada, "Study for realization of spin-polarized field effect transistor in $In_{0.75}Ga_{0.25}As/In_{0.75}Al_{0.25}As$ heterostructure," Physica E, vol. 12, pp. 399–402, 2002.

[14] K. Tomizawa, *Numerical Simulation of Submicron Semiconductor Devices*, Artech House, 1993.

[15] K. Blum, *Density Matrix Theory and Applications*, Plenum Press, 1996.

[16] G. Dresselhaus, "Spin-Orbit Coupling Effects in Zinc Blende Structures," Phys. Rev., vol. 100, pp. 580–586, 1955.

[17] M. I. Dyakonov, V. Yu. Kachorovskii, "Spin relaxation of two-dimensional electrons in noncentrosymmertic semiconductors," Sov. Phys. Semicond., vol. 20, pp. 110–112, 1986.

[18] M. V. Fischetti, S. E. Laux, *DAMOCLES Manual*, IBM, April 1995.

[19] E. A. de Andrada e Silva, G. C. La Rocca, F. Bassani, "Spin-split subbands and magneto-oscillations in III-V asymmetric heterostructures," Phys. Rev. B, vol. 50, pp. 8523–8533, 1994.

[20] M. Cardona, N. E. Christensen, G. Fasol, "Relativistic band structure and spin-orbit splitting of zinc-blende-type semiconductors," Phys. Rev. B, vol. 38, pp. 1806–1827, 1988.

[21] A. Tackeuchi, O. Wada, Y. Nishikawa, "Electron spin relaxation in InGaAs/InP multiple-quantum wells," Appl. Phys. Lett., vol. 70, pp. 1131–1133, 1997.

[22] A. Hirohata, S. J. Steinmueller, W. S. Cho, Y. B. Xu, C. M. Guertler, G. Wastlbauer, J. A. C. Bland, S. N. Holmes, "Ballistic spin filtering across ferromagnet/semiconductor interfaces at room temperature," Phys. Rev. B, vol. 66, art. no. 035330, 2002.

[23] J. Nitta, T. Akazaki, H. Takayanagi, T. Enoki, "Gate control of spin-orbit interaction in an inverted $In_{0.53}Ga_{0.47}As/In_{0.52}Al_{0.48}As$ heterostructure," Phys. Rev. Lett., vol. 78, pp. 1335–1338, 1997.